



HAL
open science

A study on transparency of a passive manipulation mechanism : application to Neoditech Scara Parts

Thomas Muller, Kévin Subrin, Sebastien Garnier, D Joncheray, A Billon

► To cite this version:

Thomas Muller, Kévin Subrin, Sebastien Garnier, D Joncheray, A Billon. A study on transparency of a passive manipulation mechanism : application to Neoditech Scara Parts. Congrès Français de Mécanique, Aug 2019, Brest, France. hal-02473209

HAL Id: hal-02473209

<https://hal.science/hal-02473209>

Submitted on 10 Feb 2020

HAL is a multi-disciplinary open access archive for the deposit and dissemination of scientific research documents, whether they are published or not. The documents may come from teaching and research institutions in France or abroad, or from public or private research centers.

L'archive ouverte pluridisciplinaire **HAL**, est destinée au dépôt et à la diffusion de documents scientifiques de niveau recherche, publiés ou non, émanant des établissements d'enseignement et de recherche français ou étrangers, des laboratoires publics ou privés.

A study on transparency of a passive manipulation mechanism : application to Neoditech Scara Parts

T. Muller^{a,b}, K. Subrin^a, S. Garnier^a, D. Joncheray^b, A. Billon^b

a. LS2N, RoMaS team, IUT Nantes, 2 Avenue du professeur Jean Rouxel, 44475 Carquefou

b. Neoditech, ZI les Roitelières, 44330 Le Pallet

Abstract :

In the field of 5 to 100 kg load transportation in workshops, many systems having more or less complex architectures have been developed to reduce musculo-skeletal disorders (hoists, pliers, dedicated systems). These systems offer different behaviors and human interaction is far from being the same for all of them. In recent years, the literature produced a lot of work around design thinking, user-centered approaches emphasizing notions around perception, cognition, and ergonomics to meet the needs of the end user. The development of cobotics and more generally systems allowing the interaction or co-manipulation of objects highlights the notion of transparency of the system. This transparency is expressed as the fact of feeling only a part of the physical magnitudes of the object most relevant to the user in his manipulation. In the context of this article, we study the transparency of a kinematically redundant passive mechanism based on a scara one (revolute joints parallel between them) when manipulating heavy objects on a plane. This article is based on a state of the art of different criteria in order to evaluate the behavior of a robot such as manipulability or dexterity. We will indicate the relevance of these criteria that we apply to a theoretical study. These theoretical aspects will then be evaluated on Neoditech Scara Parts arm. It is a mechanism capable of handling up to 50kg composed of a plane arm mounted on vertical linear axis itself mounted on a fixed or mobile base. This plane arm consists of 6 revolute joints having parallel axes ensuring redundancy in the architecture of the robot.

Keywords : Robotic ; Cobotics ; Transparency ; Manipulability analysis ; Passive Mecanisms ; Load transportation ; Scara Architecture

1 Introduction

In recent years, robotic evolved in order to improved the interaction between Human and robotic solutions. The term "Cobotic" which means collaborative robotic is an extension of robotics designed to create a synergy between humans and robots to reduce the hardness of work and improve the performance of the company. Three approaches are often presented highlighting the exoskeletons, collaborative robots (sharing of workspace) and cooperative robots (co-manipulation work). This also allows the man who works to keep his know-how related to several years of experience and also to adapt to the flexibility of the workshop. In the quest to improve productivity and reduce MSDs (musculo skeletal disorders) and their associated costs, many companies are moving towards more or less affordable cobotic solutions.

In the case of the Neoditech Scara Parts, a passive mechanism consisting of a series of revolute joints can support a load of up to 50 kg vertically movable by a remote controlled linear axis. No control law allows

here to maximize transparency or trust, only the architecture, the masses, the inertia and the coefficients of friction of the mechanism and the load have an influence on these indicators. It is known for its fluidity and transparency to its users. This article focuses on finding the causes of this reputation and evaluating them.

The performances of these robots are linked to performances similar to those of conventional robots (speed, payload, ...) but also to performances more difficult to evaluate (transparency, trust, [1]...). Many theories have been developed around the control of these robots as the impedance control [2] to make them more and more attractive to operators through the maximization of criteria such as trust, transparency, ... These control laws are often effective but require a certain number of sensors to be put in place.

However, the problems of synthesis of the mechanisms are often related to a determination of dimensions, of connections to maximize criteria like the manipulability [3], the dexterity [4], the avoidance of the singularities in a desired workspace [5]. Redundant and Hyper-redundant mechanisms are designed to answer the problematic of the maximisation of these parameters as well as the problematic of obstacle avoidance [6] [7].

In this article, we will focus on making a state of the art of mechanism indicator and we will then evaluate them on the Neoditech manipulator. Finally we will try to understand the influence of the redundancy degree on these indicators to explain the strength and weaknesses of the Neoditech manipulator.

2 Critical review of known indicators

2.1 Introduction

There are hundreds of performance indicators for robots. It is, however, necessary to extract those which interest us for our study. Indicators are generally classified into three categories : local or global, kinematic or dynamic, extrinsic or intrinsic (task related or not) according to Patel [8]. We find mostly indicators based on the workspace, the joints and the Jacobian in the literature. We will present some indicators relevant to our application that we found in the literature reviews from Patel [8] and Zhang [9].

2.2 Workspace indicators

Several types of workspaces are defined in the literature. They are shown in figure 1. Among the most relevant for our study, we find :

- The operating volume : The total volume the manipulator can reach
- The reachable position workspace : (defined by Gupta and Roth [10]) the set of points that can be reached by a reference point on a manipulator with at least one orientation and does not include singular points where the manipulator loses one or more degrees of freedom.
- The dexterous workspace [11] : The set of points of which rotation about all possible axis can be performed

2.3 Joints indicators

For the indicators on the joints, there are indicators on the speed and the position of these. The first is a ratio between the articular velocities and the speed of the effector at a weighting coefficient. It is called

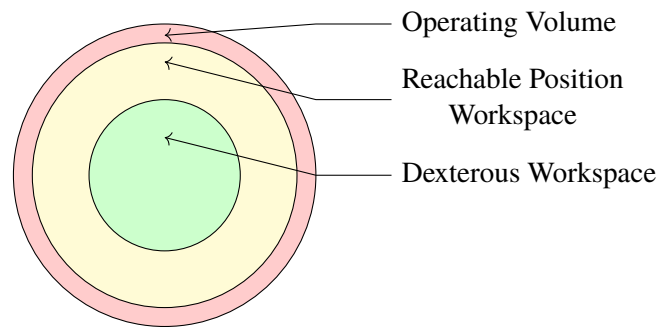


FIGURE 1 – Workspace definitions

the manipulator velocity ratio r_v , it was introduced by Dubey [12] :

$$r_v = \sqrt{\frac{\dot{x}_v^T \dot{x}_v}{\dot{\theta}_v^T \dot{\theta}_v}} \quad \text{with} \quad x_v = \sqrt{W_x} \dot{x} \quad \text{and} \quad \theta_v = \sqrt{W_\theta} \dot{\theta} \quad (1)$$

At the position level, indicators can be used to describe the distance of the joint position from the limit values (or the proximity to the central value). We thus find the Joint Range Availability *JRA* [13] and its normalized version. Another representation is the objective function of Baron [14].

However, we chose in this article not to evaluate these type of indicators because of their trajectory dependency but we are not neglecting them for future work.

2.4 Jacobian indicators

The Jacobian matrix J is very important in any mathematical representation of robotics and it is quite obvious to find it at the heart of many indicators. Its first use was made by Yoshikawa [3] for the measurement of manipulability. A zero manipulability is obviously caused by a singularity in the robot configuration.

$$\mu = \sqrt{\det(JJ^T)} \quad (2)$$

This measurement is then developed in dynamic manipulability [3] taking into account the matrices of inertia of solids M :

$$\mu_{dyn} = \sqrt{\det(J(MM^T)^{-1}J^T)} \quad (3)$$

The decomposition into singular values of the Jacobian matrix also makes it possible to judge the worst or the best kinematic transmission ability according to the directions. The worst is called minimum singular value σ_{min} [15]. In addition, we can also judge the isotropy of these ability transmission, comparing the maximum and minimum values. This indicator is also called dexterity Δ [4].

$$\mu = \sigma_1 \sigma_2 \dots \sigma_n \rightarrow \sigma_{min} = \min(\sigma_i) \quad (4) \quad \Delta = \frac{\sigma_{min}}{\sigma_{max}} \quad (5)$$

The inverse (or the inverse of Moore-Penrose in the redundant case) of the Jacobian makes it possible to determine the kinematic transmission accuracy index k and its inverse the dexterity index.

$$k = \|J\| \|J^+\| \quad (6)$$

The workspace integral of this dexterity index is used to determine the robot's Global Conditioning Index [16]. It is also possible to determine the variation of this index on the workspace with the Zhixin formulation [17]. It allows us to see the robot isotropy/anisotropy on the global workspace.

$$\eta = \frac{\int_W \frac{1}{k} dW}{\int_W dW} \quad (7)$$

$$\chi = \sqrt{\frac{\int_W (\frac{1}{k} - \eta)^2 dW}{\int_W dW}} \quad (8)$$

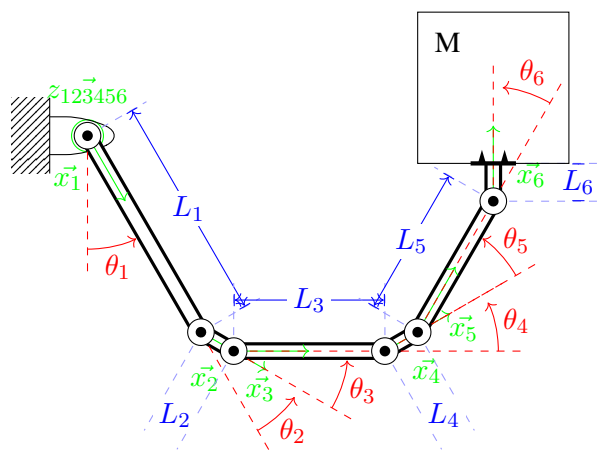
2.5 Critic of these indicators

The problem of all indicators remains most of the time their units and their dependence that make them almost incomparable between each robot. We can list the dependence on the lengths, the scale, the types of connections, the reference used, etc. To resolve these concerns, the indicators previously presented have been improved by dividing them by the sum of lengths l to the square for (2) or just by l for (4) [18]. For (5), when the dimension of the task is greater than two, a new measure is introduced in [18]:

$$\Delta_{iso} = \frac{\sqrt[n]{\sigma_1 \sigma_2 \dots \sigma_n}}{\sigma_{avg}} \quad (9)$$

3 Neoditech scara parts indicator evaluation

3.1 Parametrization



$a(mm)$	θ	d	α	$\theta_{max}(^\circ)$	$\theta_{min}(^\circ)$
$L_1 = 602$	θ_1	0	0	220	-130
$L_2 = 90$	θ_2	0	0	90	-90
$L_3 = 580$	θ_3	0	0	90	-90
$L_4 = 90$	θ_4	0	0	90	-90
$L_5 = 580$	θ_5	0	0	90	-90
$L_6 = 58$	θ_6	0	0	90	-90

FIGURE 2 – Neoditech Scara Parts parametrization

TABLE 1 – Denavit Hartenberg parameters

We can see the system on figure 5 and its parametrization on figure 2. The Denavit Hartenberg parameters

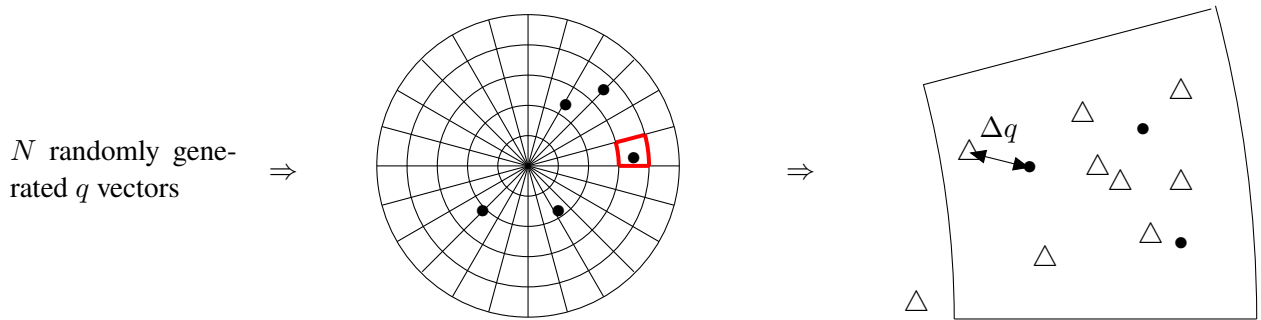


FIGURE 3 – Monte Carlo extended method

are described in the table 1. The Jacobian J in position of a plane robot like this one is written :

$$J = \begin{pmatrix} J_{12} - L_1 s_1 & J_{13} - L_2 s_{12} & J_{14} - L_3 s_{123} & J_{15} - L_4 s_{1234} & J_{16} - L_5 s_{12345} & -L_6 s_{123456} \\ J_{22} + L_1 c_1 & J_{23} + L_2 c_{12} & J_{24} + L_3 c_{123} & J_{25} + L_4 c_{1234} & J_{26} + L_5 c_{12345} & L_6 c_{123456} \end{pmatrix} \quad (10)$$

3.2 Workspace analysis

In order to analyze the workspace, we will use the extended Monte-Carlo technique as described in [19]. It consists of calculating N random positions of the effector with the forward kinematics from N random q vectors. Then we make a meshing from the potential workspace in the polar coordinate system and we associate all the positions to one center node of the meshing. The seed space being generated, we can now make it grow by adding a centered normally distributed Δq vector with a standard deviation σ being chosen. If the forward kinematics from the $q + \Delta q$ vector is still near the same node than this from q , we will add it to our list, else we will delete it. This is explained in figure 3.

For our simulation, we will take the following parameters for the meshing : 5cm for the radius and 0.25 rad for the angle which makes 1107 nodes. 5000 random points have been evaluated which have generated points in all zones of the meshing with a mean of 5 points per node. These 5000 points will generate 100 000 total points in the robot workspace.

To see if all orientations are possible for one node we will sort the orientation obtained for all the points generated in one element. If the difference between two following orientations is bigger than $\epsilon (= 0.05 \text{rad})$ we will count it as an impossibility to reach an orientation. On the figure 4, we can see in

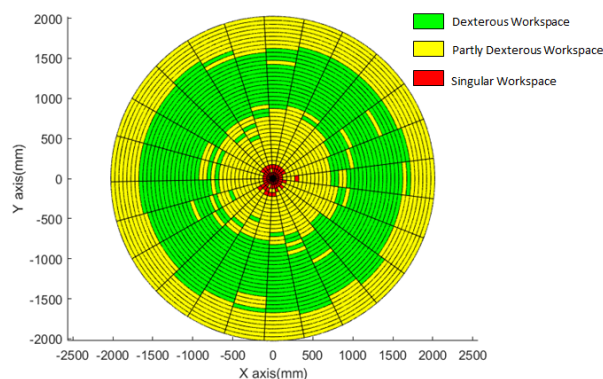


FIGURE 4 – Neoditech's Scara Parts workspace



FIGURE 5 – System studied

green where all orientations are considered as reachable, in yellow where only a part of the orientations are reachable and in red where only very little orientations are reachable.

3.3 Jacobian indicators

The Monte Carlo method generated enough points for us to evaluate the jacobian indicators in the manipulator space. However, it is not easy to represent them because there are multiple configurations for one position in space and a different indicator value for each one of these configurations. The representation (x,y,indicator) is therefore not adapted because of its readability. We can also prove that all indicators we presented do not depend from q_1 and that the q_1 range is almost 360 degrees. This both properties allows us to jump to a (r,indicator) representation which is more readable. We will thus choose to represent this solution space in the 2D form of level lines between the maximum and minimum values of the chosen indicator. A scale represents the repartition of manipulabilty for the same radiuses.

3.3.1 Manipulability

On the figure 6 we can see the manipulability of the Neoditech Scara Parts and its normalized version. We can clearly see the zone between 900 and 1700 mm of radius in which he is the most manipulable. This is also the zone where he is recommended to be used . There a some spikes of bad manipulability corresponding to singularity configurations but globally 70 % of the values are over 50 % of the maximum value. The zero manipulability is achievable in almost every radius of the robot workspace which is a sign that the singularity space is a five dimension space depending of the θ_2 to θ_6 values. This space can only be evaluated numerically for this type of robot because it depends of very long trigonometric equations.

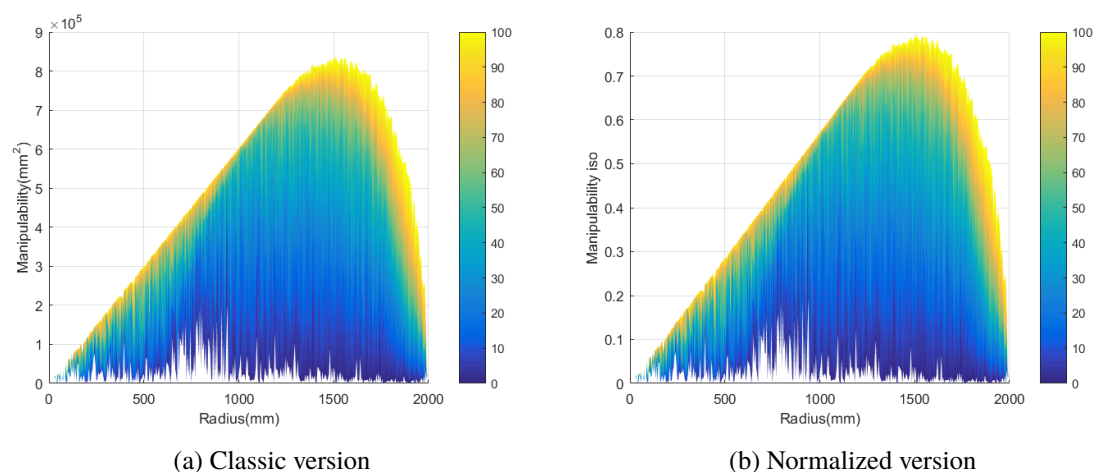


FIGURE 6 – Neoditech manipulability indicator

3.3.2 Minimum Velocity

On the figure 7, the minimum velocity of the jacobian is represented with its normalized version. We can see that the lowest velocity minimums happens at the high radiuses. This cause a lack of transparency because the user can only move the effector in one direction. The graphs also shows that at 1000 mm we have the lowest chances to be in this kind of configuration.

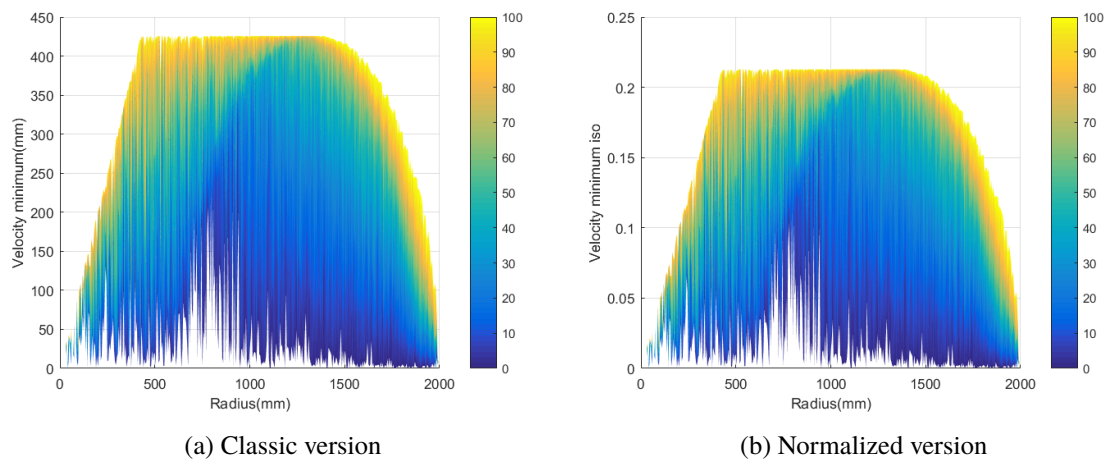


FIGURE 7 – Neoditech minimum velocity

3.3.3 Dexterity

On the figure 8, the dexterity is shown with its normalized version. The dexterity is maximal at 500 mm and it decreases until zero at 2000 mm. However for the normalized and the classic version the decrease inclination is not the same. While for the classic version it is very violent at first and less pronounced on the end, we find the opposite for the standardized version. If we comment the normalized version which is supposed to be the most objective one, we have a very good dexterity until 1700 mm that is too put in correlation with the classic version.

The mean of the classic and the normalized version of the global conditioning indicator are at 0.165 and 0.629 . It tells us that the manipulator is globally isotropic if we take in account the normalized version. The zhixin indicator has a value of 0.122 and 0.200, it is a sign of great sparsity for the dexterity because this indicator is like a standard deviation indicator for the dexterity.

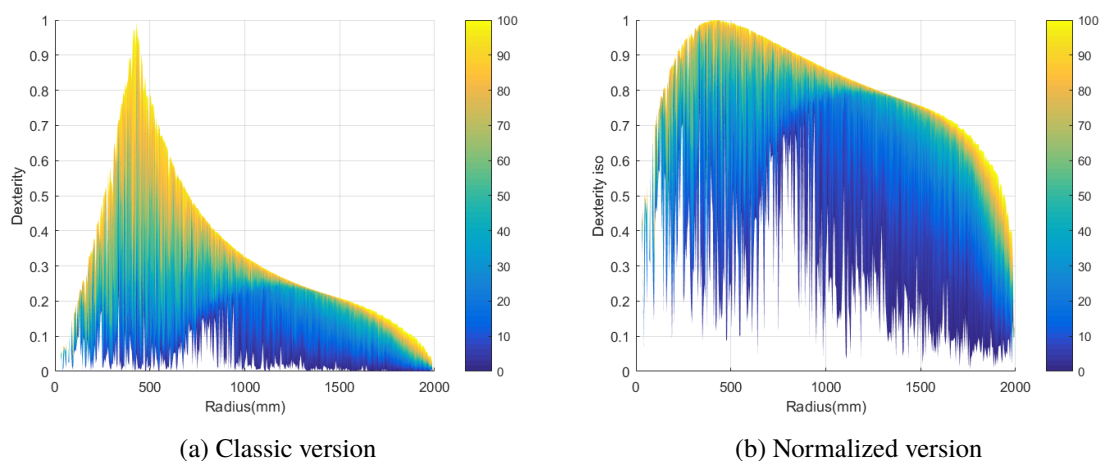


FIGURE 8 – Neoditech dexterity

4 Contribution of architecture on these indicators

In the previous part, we applied the different criteria set out in part 2 on our system, but that did not allow us to answer the question : what makes it a better system than a manipulation arm at 2,3 or n connections ? To try to make a comparison between these different architectures, we will try to compare the values of the previous indicators for robots with n consecutive links with arm lengths of $2/n$ meters for n ranging from 2 to 6. We will then try to vary these lengths to approach the configuration of Neoditech which has rotationnal joints arranged in a non regular way. The joints limits considered will be none for the first axis and ± 90 degrees for all the other axis. The Table 2 presents the robot, that will be evaluated in this article.

Robot Name	Number of Revolute Joints	Lengths (m)
R2-Iso	2	$L_1 = L_2 = 1$
R2-C1	2	$L_1 = 1.5, L_2 = 0.5$
R2-C2	2	$L_1 = 0.5, L_2 = 1.5$
R3-Iso	3	$L_1 = L_2 = L_3 = 0.66$
R3-C1	3	$L_1 = 0.9, L_2 = 0.2, L_3 = 0.9$
R4-Iso	4	$L_1 = L_2 = L_3 = L_4 = 0.5$
R4-C1	4	$L_1 = 0.8, L_2 = 0.2, L_3 = 0.8, L_4 = 0.2$
R5-Iso	5	$L_1 = L_2 = L_3 = L_4 = L_5 = 0.4$
R6-Iso	6	$L_1 = L_2 = L_3 = L_4 = L_5 = L_6 = 0.33$

TABLE 2 – Configurations of robot evaluated

4.1 Workspace

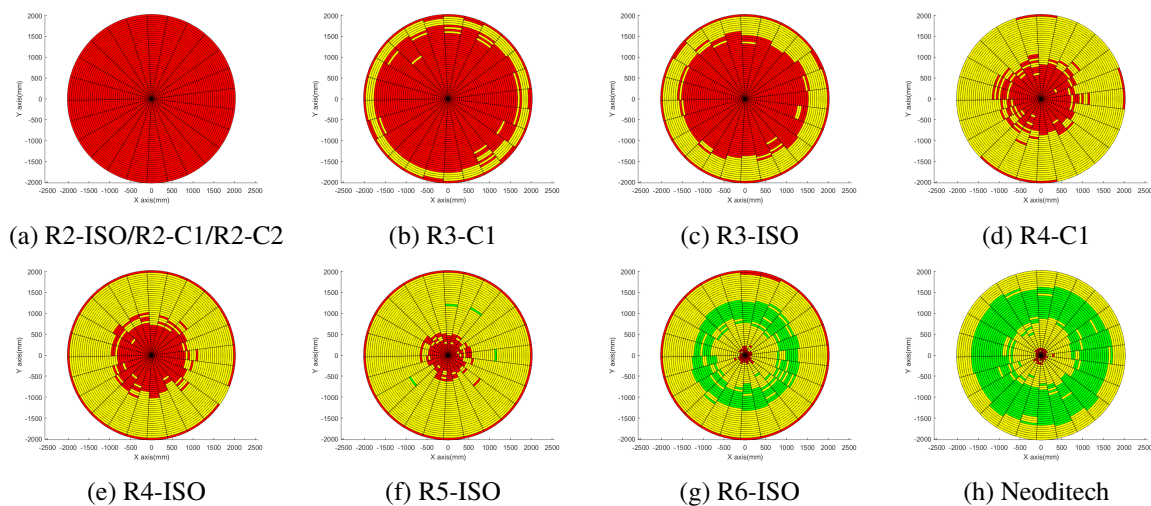


FIGURE 9 – Workspaces associated to each robot

The same indicators than in 3. were evaluated on the robot previously presented. On the figure 9, we can see the results obtained for the workspaces. They show the increase of the dexterous workspace with the degrees of freedom from the R2 configuration where only 2 orientations are available to the R6 configuration where almost all orientations are available in a space. We can also conclude that the apparition of the dexterous workspace is only possible for manipulators of this type with 4 or more degrees of freedom. The anisotropic configurations are less performant than the isotropic except for the Neoditech which seems to increase the dexterous workspace at higher radiuses. The conclusion for this

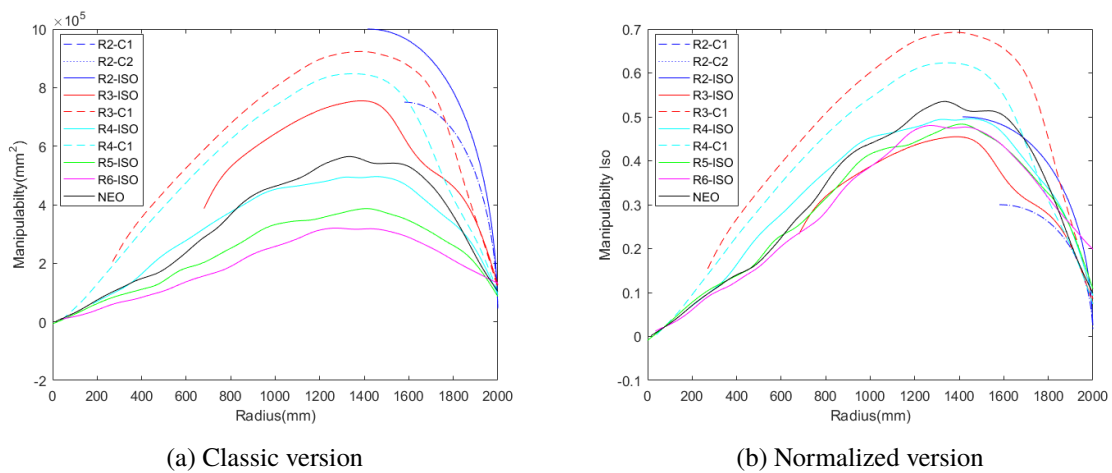


FIGURE 10 – Manipulability of each robot

part is that we can always increase the joints number to make our space more dexterous but the length variation is a cheaper opportunity to shift the dexterous workspace at a desired location which is relevant for the application.

4.2 Jacobian indicators

To compare the different indicators, we chose to draw only the mean on the radius of all the indicators, in contrary to the previous part where we drew all the surface from minimum to maximum.

4.2.1 Manipulability

In terms of manipulability, the figure 10 indicates that the manipulability generally decreases when the number of joints rises. This tells us, firstly the problem of isotropy of this measure. For the other arm configuration, the anisotropy generally increases the manipulability except for the 2 joints arm which has the same values for each configuration.

The normalized version of the manipulability shows very close results for the isotropic manipulators

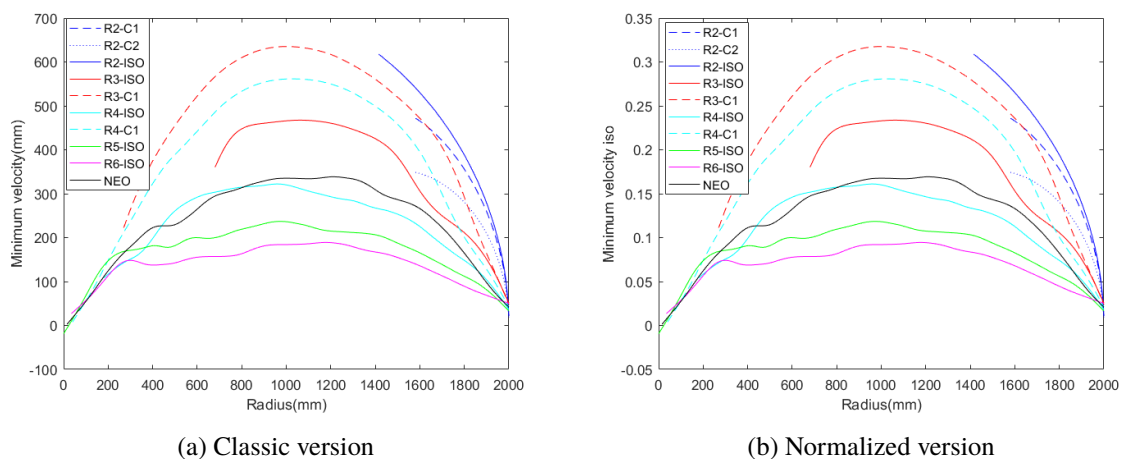


FIGURE 11 – Minimum velocity of each robot

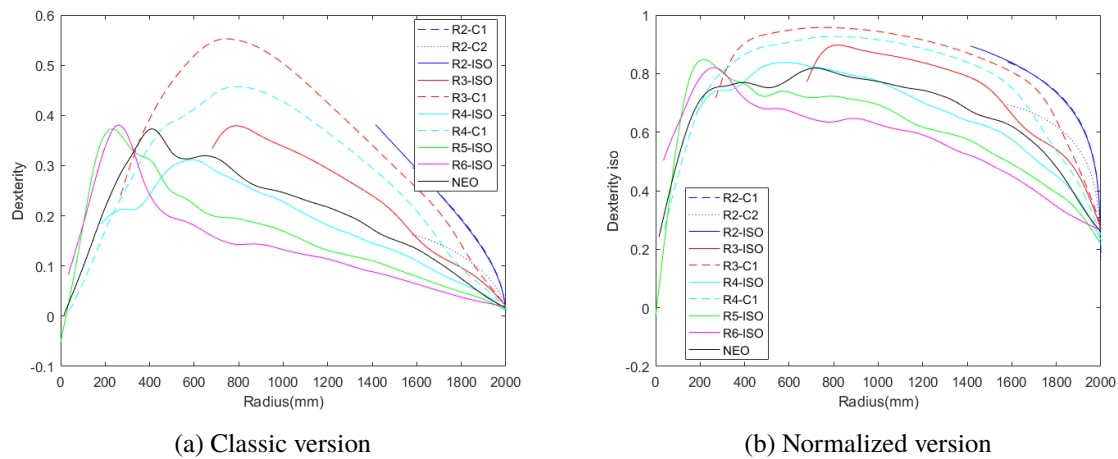


FIGURE 12 – Dexterity of each robot

which is a sort of reference to compare to other architectures. Both anisotropic architectures have the same behavior than before, they have higher manipulability than the isotropic architectures.

4.2.2 Minimum Velocity

The minimum velocity shown in figure 11 the increase in the number of degrees of freedom generally cause a decrease of it. It is explained by the increasing number of singular positions of the manipulator. The anisotropic configurations generally have a higher minimum velocity than isotropic configurations. This is also the case for the Neoditech compared to R4,R5 and R6-ISO.

4.2.3 Dexterity

Finally, for the dexterity(figure 12) the conclusions are similar to those for the minimum velocity. The normalized version of the indicator gives closer values between all the manipulators than the classic one but the classification of the manipulator is approximately the same .

The global conditioning index helps us to compare the manipulator more easily than the dexterity graphs. In the table 3 , the results for the different robots are shown. The Neoditech has one of the best global conditioning index of the manipulators presented for his workspace. However, the Zhixin indicator shows that the dexterity distribution is more extended than for the other manipulators. This may cause a bad feeling to the users because it corresponds too a widespreaded repartition of the manipulator ability to move in several directions.

Robot	R2-ISO	R2-C1	R2-C2	R3-ISO	R3-C1	R4-ISO	R4-C1	R5-ISO	R6-ISO	Neoditech
η	0.171	0.141	0.088	0.137	0.209	0.118	0.192	0.099	0.095	0.165
η_{iso}	0.643	0.605	0.511	0.594	0.665	0.565	0.658	0.522	0.509	0.629
χ	0.108	0.085	0.048	0.090	0.157	0.076	0.135	0.076	0.080	0.122
χ_{iso}	0.201	0.187	0.158	0.192	0.226	0.181	0.212	0.177	0.175	0.200

TABLE 3 – GCI and Zhixin indicator of each robot

5 Conclusion

This article presents a co-manipulation system used in industry as well as various indicators that are evaluated. The application of various methodologies from the literature are put in place to evaluate this system. Finally, this article tries to link the practicality of this architecture compared to other conceivable.

Nevertheless, this article scans only a few indicators that can be evaluated purely theoretically. In our future work, we will endeavor to evaluate the system in a more experimental way using typical trajectory implementations of this system. We can then observe the indicators on the joints but also look at the correlation between force exerted by the operator and real displacement which is the first definition of transparency. The study of the use of joint ranges and singularities should also not be neglected.

Nomenclature

Δ	Dexterity
η	Global Conditioning Index
μ	Minimum Velocity
μ	Yoshikawas Manipulability
μ_{dyn}	Yoshikawa dynamic manipulability
σ_i	Singular values from a matrix
θ	Joint position vector
$c_{ij}(s_{ij})$	sum of cosine (sine) of q_i and q_j
J	Jacobian matrix
J^+	Moore-Penrose inverse from the jacobian matrix $((J^T J)^{-1} J^T)$
L_i	Length of an arm
M	Matrix of inertia from the robot
W	Manipulator Workspace
$W_{\theta,x}$	Weighting matrices
x	Effector position vector
X_{iso}	Isotropic measure of X
χ	Global Conditioning Index anisotropy

Références

- [1] J. Lyons, “Being Transparent about Transparency : A Model for Human-Robot Interaction,” in *2013 AAAI Spring Symposium Series*, Mar. 2013.
- [2] A. Freedy, E. DeVisser, G. Weltman, and N. Coeyman, “Measurement of trust in human-robot collaboration,” in *2007 International Symposium on Collaborative Technologies and Systems*, (Orlando, FL), pp. 106–114, IEEE, May 2007.
- [3] T. Yoshikawa, “Manipulability of Robotic Mechanisms,” *The International Journal of Robotics Research*, vol. 4, pp. 3–9, June 1985.
- [4] J. K. Salisbury and J. J. Craig, “Articulated Hands : Force Control and Kinematic Issues,” *The International Journal of Robotics Research*, vol. 1, pp. 4–17, Mar. 1982.
- [5] L. Nouaille, *Démarche de conception de robots médicaux : application à un robot de télé-échographie*. thesis, Orléans, Dec. 2009.
- [6] G. S. Chirikjian and J. W. Burdick, “Hyper-redundant robot mechanisms and their applications,” in *Proceedings IROS '91 :IEEE/RSJ International Workshop on Intelligent Robots and Systems '91*, pp. 185–190 vol.1, Nov. 1991.
- [7] K. Subrin, L. Sabourin, G. Gogu, and Y. Mezouar, “Performance Criteria to Evaluate a Kinematically Redundant Robotic Cell for Machining Tasks,” *Applied Mechanics and Materials (Volume 162)*, pp. 413–422, 2012.
- [8] S. Patel and T. Sobh, “Manipulator Performance Measures - A Comprehensive Literature Survey,” *Journal of Intelligent & Robotic Systems*, vol. 77, pp. 547–570, Mar. 2015.
- [9] P. Zhang, Z. Yao, and Z. Du, “Global Performance Index System for Kinematic Optimization of Robotic Mechanism,” *Journal of Mechanical Design*, vol. 136, pp. 031001–031001–11, Dec. 2013.
- [10] K. C. Gupta and B. Roth, “Design Considerations for Manipulator Workspace,” *Journal of Mechanical Design*, vol. 104, pp. 704–711, Oct. 1982.
- [11] R. Vijaykumar, M. Tsai, and K. Waldron, “Geometric optimization of manipulator structures for working volume and dexterity,” in *1985 IEEE International Conference on Robotics and Automation Proceedings*, vol. 2, pp. 228–236, Mar. 1985.
- [12] R. Dubey and J. Luh, “Redundant robot control for higher flexibility,” in *1987 IEEE International Conference on Robotics and Automation Proceedings*, vol. 4, pp. 1066–1072, Mar. 1987.
- [13] A. Liegeois, “Automatic Supervisory Control of the Configuration and Behavior of Multibody Mechanisms,” *IEEE Transactions on Systems, Man, and Cybernetics*, vol. 7, pp. 868–871, Dec. 1977.
- [14] L. Baron, “A Joint-Limits Avoidance Strategy for Arc-Welding Robots,” *Ecole Polytechnique Montréal*.
- [15] C. A. Klein and B. E. Blaho, “Dexterity Measures for the Design and Control of Kinematically Redundant Manipulators,” *The International Journal of Robotics Research*, vol. 6, no. 2, pp. 72–83, 1987.
- [16] C. Gosselin and J. Angeles, “A Global Performance Index for the Kinematic Optimization of Robotic Manipulators,” *Journal of Mechanical Design*, vol. 113, pp. 220–226, Sept. 1991.
- [17] Zhixin, “On Global Performance Indices of Robotic Mechanisms,” *en.cnki.com.cn*, May 2005.
- [18] K. Khosla, “Dexterity measures for design and control of manipulators,” in *IEEE/RSJ International Workshop on Intelligent Robots and Systems '91*, pp. 758–763 vol.2, Nov. 1991.
- [19] Z. Zhao and S. He, “Workspace Analysis for a 9-DOF Hyper-redundant Manipulator Based on An Improved Monte Carlo Method and Voxel Algorithm,” in *2018 IEEE International Conference on Mechatronics and Automation (ICMA)*, pp. 637–642, 2018.